Journal of Sound and Vibration (2000) **233**(2), 179–194
doi:10.1006/jsvi.1999.2810, available online at http://www.idealibrary.com on IDEAL®

FREQUENCY-RESPONSE CHARACTERISTICS OF A SINGLE-LINK FLEXIBLE JOINT MANIPULATOR AND POSSIBLE TRAJECTORY TRACKING

H. DIKEN

Mechanical Engineering Department, King Abdulaziz University, Jeddah, Saudi Arabia

(*Received* 16 *July* 1998, *and in final form* 21 *September* 1999)

A single-link manipulator consisting of servomotor, elastic shaft and rigid link is chosen to represent an elastic control system. Equations of the torsional elastic system are derived including the servomotor control system parameters. The transfer function of the elastic control system is obtained including not only control system parameters but also the natural frequency and the damping ratio of the torsional vibratory system. Non-dimensional parameters such as the ratio of the structural natural frequency to the substructural natural frequency and the ratio of the substructural natural frequency to the control system frequency are defined. The effects of these parameters on the frequency response of the system are investigated. A simple and effective method using the frequency-response characteristics is proposed to track a cycloidal trajectory precisely.

1. INTRODUCTION

Servomotors and stepper motors are rapidly replacing conventional ones. Introduction of servomotors has increased the importance of the transient motion. Transient response analysis is becoming increasingly important and critical in the design of automated machine this is why position control of mechanical systems with structural flexibility has been an important research area in recent years. Location of points at their extremities must often be controlled with great precision, by torquing at some other point separated from the first by flexible sections in structures such as manipulators, satellites, or space structures [1]. For a broad class of industrial robots, the elastic compliance is mainly concentrated in joints and harmonic drives, and for this reason there is a growing interest in the area of modelling and control of flexible joint robots and space structures. Torsionally flexible control systems have been studied by several researchers. The main emphasis has been on the adaptive control of the system. Generally, state space models are developed and linear quadratic optimal control techniques used, and robustness and stability of flexible systems are discussed [2–9]. Previously, a model similar to the one used in this paper was studied [10], with the effect of the flexibility on the poles of the control system being discussed for a specific problem. It is shown that, because of the flexibility, complex roots appear near the imaginary axis and dominate the behaviour of the system. These dominant roots change location, depending on the gains K_p, K_d and K_i. Ankarali and Diken [11] analyzed a similar problem without control and discuss conditions to eliminate the residual vibration.

In this paper, the problem is more generalized. Non-dimensional parameters such as μ, which is the ratio of the structural natural frequency to the substructural natural frequency, and λ, which is the ratio of the substructural natural frequency to the control system frequency are defined and the transfer function of the control system is obtained as the

0022-460X/00/220179 + 16 $35.00/0

function of these parameters. Frequency response of the elastic control system is analyzed with respect to these parameters. The measure of the flexibility of the control system is also given with respect to these parameters. It is shown that for low control damping ζ, an elastic control system behaves like a two-degrees-of-freedom torsional system excited with the torque at the motor side. For high values of control damping, the system behaves like a single-degree-of-freedom torsional system clamped at the motor side and free at the load side. The possible trajectory tracking with the elastic control system is also discussed. For this purpose, a cycloidal input function, which consists of one ramp and one sinusoidal part, is proposed as an input trajectory. The sinusoidal part of the cycloid is modified by using the frequency-response characteristics of the chosen system and the condition for precise trajectory tracking is obtained for the elastic control system.

2. FORMULATION

The elastic control system considered here is a servomotor attached to the manipulator link by a flexible shaft as shown in Figure 1. The gear train or harmonic drive is represented by a gear ratio n, but inertial effects are neglected. The elastic shaft has flexibility k, and damping coefficient c. The motor inertia and load inertia are represented by J_m and J_L respectively. The friction at the bearings is neglected, but if it is not neglected it can be compensated through controller gains. For this two-degrees-of-freedom vibratory system, the dynamic equations, after Laplace transformation are

$$\begin{bmatrix} \frac{J_m}{n^2}s^2 + cs + k & -(cs+k) \\ -(cs+k) & J_L s^2 + cs + k \end{bmatrix} \begin{bmatrix} n\theta_m(s) \\ \theta_L(s) \end{bmatrix} = \begin{bmatrix} T(s)/n \\ 0 \end{bmatrix}. \tag{1}$$

Here θ_m and θ_L show the angular motion of the motor and the load respectively. T is the torque applied to the motor side. For a PD position control of the servomotor shown in Figure 2 [12], without considering torque disturbances, the torque produced to drive the system can be obtained as

$$\frac{T(s)}{n} = \frac{K_T K_p + K_T K_d s}{R_a n^2}\theta_d(s) - \frac{K_T K_p + K_T(K_d + K_b)s}{R_a n^2} n\theta_m(s), \tag{2}$$

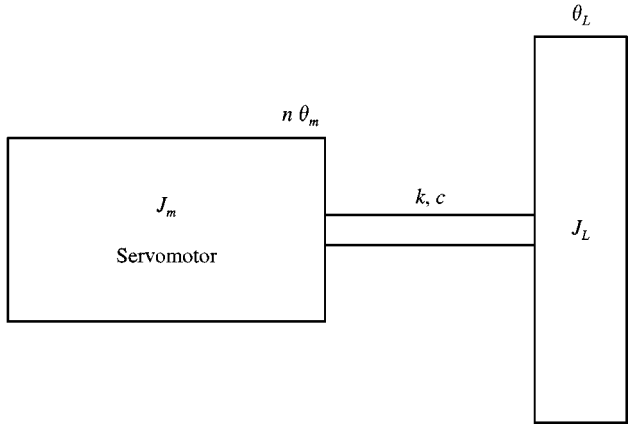

Figure 1. The model of the elastic control system.

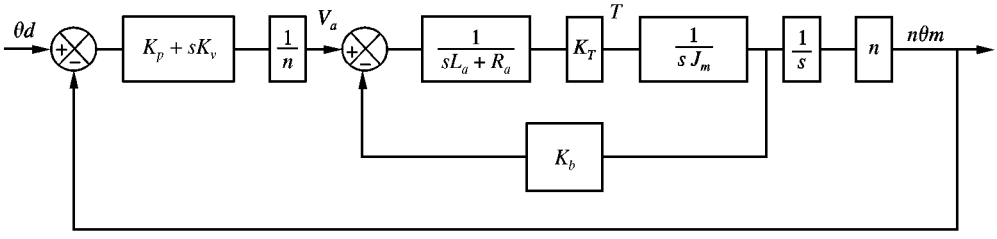

Figure 2. Block diagram of the servomotor control system.

where K_p and K_d are proportional and derivative gain constants respectively. L_a is the armature inductance and usually much smaller than R_a, and here the effect of L_a can be neglected. R_a is the resistance of the armature coils, K_T is the torque constant, K_b is the back electromotive force constant, and θ_d is the desired angular motion. When equation (2) is inserted in equation (1), the following relation is obtained:

$$\begin{bmatrix} \frac{J_m}{n^2}s^2 + cs + k + \frac{K_T K_p + K_T(K_d + K_b)s}{R_a n^2} & -(cs + k) \\ -(cs + k) & J_L s^2 + cs + k \end{bmatrix} \begin{bmatrix} n\theta_m(s) \\ \theta_L(s) \end{bmatrix}$$

$$= \begin{bmatrix} \frac{K_T K_p + K_T K_d s}{R_a n^2}\theta_d(s) \\ 0 \end{bmatrix}. \tag{3}$$

Using equation (3), the transfer function of the control system relating the output angular motion to the desired input angular motion is obtained as

$$\frac{\theta_L(s)}{\theta_d(s)} = \frac{\frac{2\zeta_n}{\omega_n T_d}s^2 + \left(\frac{2\zeta_n}{\omega_n T_p} + \frac{1}{T_d}\right)s + \frac{1}{T_p}}{\frac{1}{\omega_n^2}s^4 + \left[\frac{2\zeta_n}{\omega_n} + \frac{1}{\omega_L^2}\left(\frac{1}{T_d} + \frac{1}{T_m}\right)\right]s^3 + \left[1 + \frac{1}{\omega_L^2}\frac{1}{T_p} + \frac{2\zeta_n}{\omega_n}\left(\frac{1}{T_d} + \frac{1}{T_m}\right)\right]s^2} \tag{4}$$

$$+ \left(\frac{2\zeta_n}{\omega_n}\frac{1}{T_p} + \frac{1}{T_d} + \frac{1}{T_m}\right)s + \frac{1}{T_p}.$$

Definitions of the terms appearing in this transfer function are

$$T_m = \frac{R_a(J_m + n^2 J_L)}{K_T K_b}, \tag{5}$$

$$T_p = \frac{R_a(J_m + n^2 J_L)}{K_T K_p}, \qquad T_d = \frac{R_a(J_m + n^2 J_L)}{K_T K_d}, \tag{6}$$

$$\omega_n = \sqrt{\frac{J_m + n^2 J_L}{J_m J_L}}\,k, \quad \zeta_n = \frac{c}{2k}\omega_n, \quad \omega_L = \sqrt{\frac{k}{J_L}}. \tag{7}$$

Here T_m is the motor mechanical time constant, T_p and T_d are the parameters related to the proportional gain and derivative gain, ω_n is the structural natural frequency, ζ_n is the

structural damping ratio, and ω_L is the substructural natural frequency of the torsionally flexible system. Here a substructure is defined as a flexible system which is obtained by fixing the motor end of the flexible shaft while keeping the link side free to rotate. If the shaft is assumed to be rigid, ω_n and ω_L will go to infinity and the elastic system transfer function will be reduced to the rigid system transfer function:

$$\frac{\theta_L(s)}{\theta_d(s)} = \frac{\left(\frac{1}{T_d}s + \frac{1}{T_p}\right)}{\left(s^2 + \left(\frac{1}{T_m} + \frac{1}{T_d}\right)s + \frac{1}{T_p}\right)}. \tag{8}$$

If K_T is assumed to be zero for no control torque, then T_d, T_p, and T_m will go to infinity and the characteristic equation of the system will reduce to

$$s^2(s^2 + 2\zeta_n\omega_n s + \omega_n^2) = 0 \tag{9}$$

which gives the rigid-body motion and the characteristic equation of the two-degrees-of-freedom torsionally flexible system. Equation (8) can also be written in the following form [13]:

$$\frac{\theta_L(s)}{\theta_L(s)} = \frac{\left(\frac{\omega^2}{z}s + \omega^2\right)}{(s^2 + 2\zeta\omega s + \omega^2)}. \tag{10}$$

Here

$$\omega^2 = \frac{1}{T_p}, \quad 2\zeta\omega = \frac{1}{T_m} + \frac{1}{T_d}, \quad z = \frac{K_p}{K_d}. \tag{11}$$

If the system were rigid, ω and ζ would be the rigid control system frequency and damping ratio respectively. With the above definitions, the transfer function of the elastic control system given in equation (4) becomes

$$\frac{\theta_L(s)}{\theta_d(s)} = \frac{\left[\left(\frac{2\zeta_n}{\mu\omega_L}\frac{\omega^2}{z}\right)s^2 + \left(\frac{2\zeta_n}{\mu\omega_L}\omega^2 + \frac{\omega^2}{z}\right)s + \omega^2\right]}{\left[\left(\frac{1}{\mu^2\omega_L^2}\right)s^4 + \left(\frac{2\zeta_n}{\mu\omega_L} + \frac{1}{\omega_L^2}2\zeta\omega\right)s^3 + \left(1 + \frac{\omega^2}{\omega_L^2} + \frac{2\zeta_n}{\mu\omega_L}2\zeta\omega\right)s^2 + \left(\frac{2\zeta_n}{\mu\omega_L}\omega^2 + 2\zeta\omega\right)s + \omega^2\right]} \tag{12}$$

Here μ is defined as the ratio between the structural natural frequency and the substructural natural frequency of the torsionally flexible system. It is also a function of the inertia ratio:

$$\mu = \frac{\omega_n}{\omega_L} = \sqrt{1 + \frac{n^2 J_L}{J_m}}. \tag{13}$$

If $s = j\omega_r$ and the substructural frequency ratio $\lambda = \omega_L/\omega$, and the resonance frequency ratio $r = \omega_r/\omega$, then the magnitude and phase angle for the frequency response of the elastic control system become

$$M = \left|\frac{\theta_L(j\omega_r)}{\theta_d(j\omega_r)}\right| =$$

$$\sqrt{\frac{\left(1 - \frac{2\zeta_n}{\mu\lambda}\frac{r^2}{\beta}\right)^2 + \left(\frac{2\zeta_n}{\mu\lambda} + \frac{1}{\lambda}\right)^2 r^2}{\left[1 - \left(1 + \frac{1}{\lambda^2} + \frac{2\zeta_n}{\mu\lambda}2\zeta\right)r^2 + \frac{r^4}{\mu^2\lambda^2}\right]^2 + \left[\left(2\zeta + \frac{2\zeta_n}{\mu\lambda}\right)r - \left(\frac{2\zeta_n}{\mu\lambda} + \frac{2\zeta}{\lambda^2}\right)r^3\right]^2}}, \tag{14}$$

$$\phi = \tan^{-1}\frac{\left(\frac{2\zeta_n}{\mu\lambda} + \frac{1}{\beta}\right)r}{\left(1 - \frac{2\zeta_n}{\mu\lambda}\frac{r^2}{\beta}\right)} - \tan^{-1}\frac{\left(2\zeta + \frac{2\zeta_n}{\mu\lambda}\right)r - \left(\frac{2\zeta_n}{\mu\lambda} + \frac{2\zeta}{\lambda^2}\right)r^3}{1 - \left(1 + \frac{1}{\lambda^2} + \frac{2\zeta_n}{\mu\lambda}2\zeta\right)r^2 + \frac{r^4}{\mu^2\lambda^2}}. \tag{15}$$

When the structural damping ζ_n is ignored, the magnitude and phase angle become

$$M = \left|\frac{\theta_L(j\omega_r)}{\theta_d(j\omega_r)}\right| =$$

$$\sqrt{\frac{1 + \left(\frac{r}{\beta}\right)^2}{\left[1 - \left(1 + \frac{1}{\lambda^2}\right)r^2 + \frac{r^4}{\mu^2\lambda^2}\right]^2 + \left[(2\zeta)\left(1 - \frac{r^2}{\lambda^2}\right)r\right]^2}}, \tag{16}$$

$$\phi = \tan^{-1}\frac{r}{\beta} - \tan^{-1}\frac{(2\zeta)\left(1 - \frac{r^2}{\lambda^2}\right)r}{1 - \left(1 + \frac{1}{\lambda^2}\right)r^2 + \frac{r^4}{\mu^2\lambda^2}}. \tag{17}$$

Here $\beta = z/\omega$. Since z is the ratio of K_p and K_d, when the ω and ζ of the control system are selected, it is no longer an independent parameter. By using the definitions in equations (6) and (11), β becomes

$$\beta = \frac{\omega}{\left(2\zeta\omega - \frac{1}{T_m}\right)} = \frac{1}{\left(2\zeta - \frac{1}{\omega\mu^2 T_{mo}}\right)} \approx \frac{1}{2\zeta}. \tag{18}$$

Here T_{mo} is the time constant of the servomotor alone. Since the control system frequency ω is usually much greater than 1, μ is always greater than 1, and the control system damping ζ is generally between 0·7 and 1, then the second term will always be much less than 2ζ and

can be neglected. Equations (16) and (17) then become

$$M = \left|\frac{\theta_L(j\omega_r)}{\theta_d(j\omega_r)}\right| = \sqrt{\frac{1 + (2\zeta r)^2}{\left[1 - \left(1 + \frac{1}{\lambda^2}\right)r^2 + \frac{r^4}{\mu^2\lambda^2}\right]^2 + \left[(2\zeta)\left(1 - \frac{r^2}{\lambda^2}\right)r\right]^2}}, \tag{19}$$

$$\phi = \tan^{-1} 2\zeta r - \tan^{-1} \frac{(2\zeta)\left(1 - \frac{r^2}{\lambda^2}\right)r}{1 - \left(1 + \frac{1}{\lambda^2}\right)r^2 + \frac{r^4}{\mu^2\lambda^2}}. \tag{20}$$

As can be seen from equations (14) and (15), when λ goes to infinity (in other words, if the system is rigid), then the equations for the frequency response of the elastic control system reduce to that of the rigid control system. In these equations there are two important parameters, μ and λ, which have been defined earlier. Considering the denominator of equation (19), if the control damping ratio ζ goes to zero, the second term disappears and the first term gives two roots for the resonance depending on the values of λ and μ. For the increasing values of λ, resonance frequency approaches $r = 1$ or $\omega_r = \omega$. In other words, if $\omega_L \gg \omega$ the system behaves like a rigid system. If ζ goes to infinity, the resonance frequency becomes equal to the substructural frequency ω_L. Therefore, for very high values of ζ the motor side behaves like a fixed end and the system behaves like a flexible shaft and disc with fixed–free end conditions. The physical interpretation is such that for the low values of the control system damping ζ, the system behaves like a two-degrees-of-freedom torsionally vibratory system with J_m and J_L and is also excited with the control system torque which is a function of ζ and ω. For the high values of ζ the system behaves like a single-degree-of-freedom vibratory system fixed at the motor side and free to vibrate at the load side. Here the control system damping ζ acts as a measure of the freedom of the motor side. $\zeta = 0$ means that the motor side is free, $\zeta = \infty$ means that the motor side is clamped. This is explained in Figure 3. For $\zeta = 0{\cdot}4$ two resonance peaks are seen; one is close to 1 and the second is close to the frequency ratio $\omega_n/\omega = 4{\cdot}24$. For $\zeta = 1{\cdot}5$ the resonance frequency ratio approaches the substructural frequency ratio $\lambda = \omega_L/\omega = 3$. Figures 4–6 also show the frequency response of the elastic control system for different values of λ. In each figure the response of the system for different ζ values are also plotted. The magnitude of the frequency response decreases for growing values of λ. There is also a common point through which the responses for all values of ζ pass. The polynomal giving the r value of that point can be obtained by inserting $\zeta = 0$ and ∞ into equation (16) and equating them to each other. The polynomial is

$$\left(\frac{1}{\mu^4\lambda^4}\right)r^6 - \left(\frac{2}{\mu^2\lambda^2} + \frac{2}{\mu^2\lambda^4}\right)r^4 + \left(\frac{2}{\mu^2\lambda^2} + \frac{2}{\lambda^2} + 1\right)r^2 - 2 = 0. \tag{21}$$

The following formula also gives a good approximation to the value of r with an average error of 2%:

$$r = \sqrt{\frac{2}{\frac{1}{\mu\lambda^2} + \frac{1}{\lambda^2} + 1}}. \tag{22}$$

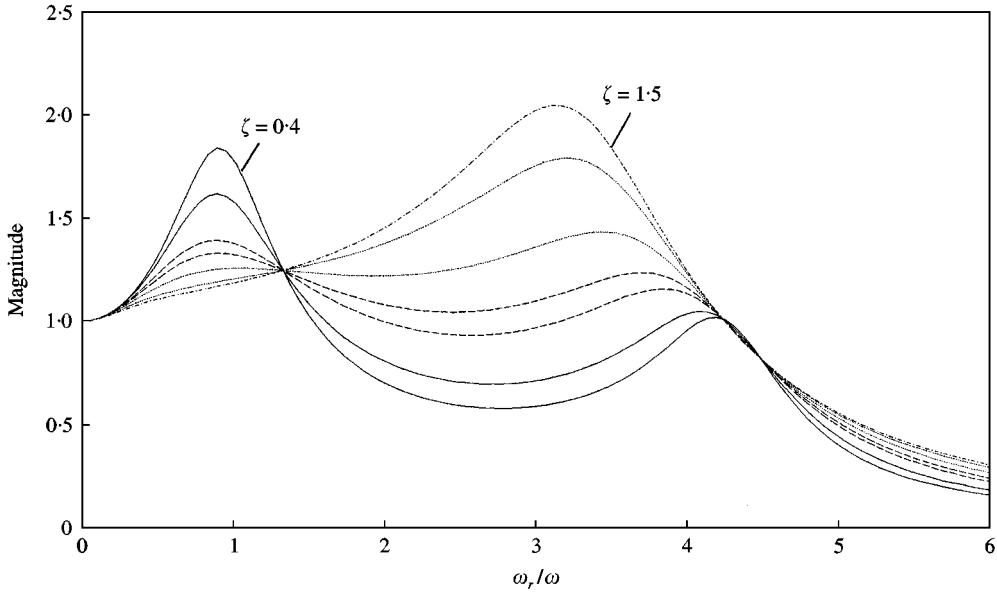

Figure 3. Frequency-response plot for $\mu = \sqrt{2} = 1{\cdot}41$, $\lambda = 3$.

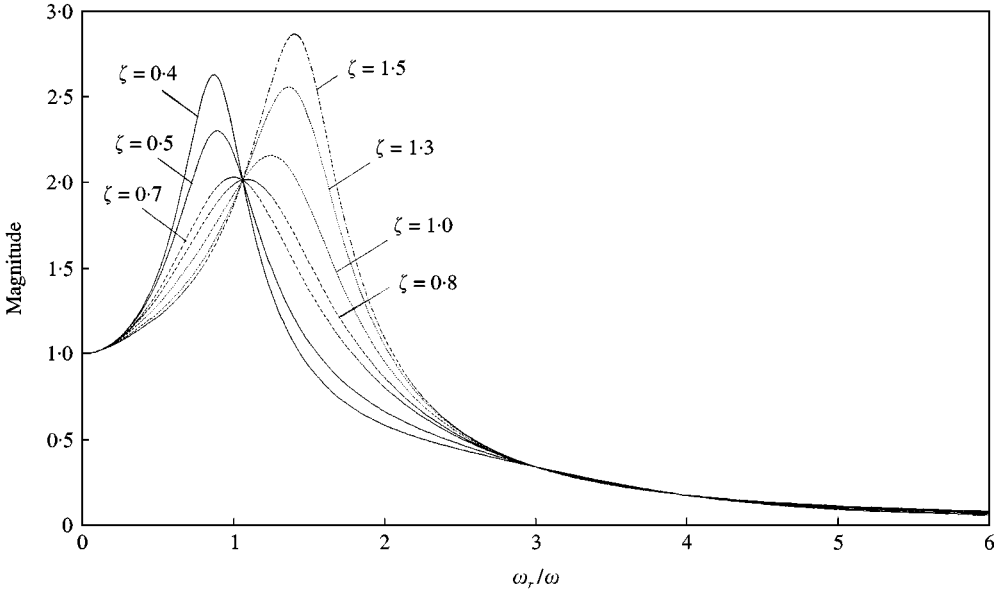

Figure 4. Frequency-response plot for $\mu = \sqrt{4} = 2$, $\lambda = 1{\cdot}5$.

It can also be seen that there is a certain value of ζ at which the maximum value of the magnitude is the least. It is difficult to find an analytical formula giving ζ for that point. Figures 7 and 8 are plotted to show the effect of λ and μ on the maximum magnitudes of the frequency responses of the elastic control system with respect to ζ. Figure 7 is plotted for different λ values. For low values of λ, the resonance frequency responses are higher and decrease with increasing values of λ. The ζ value giving the lowest maximum magnitude of

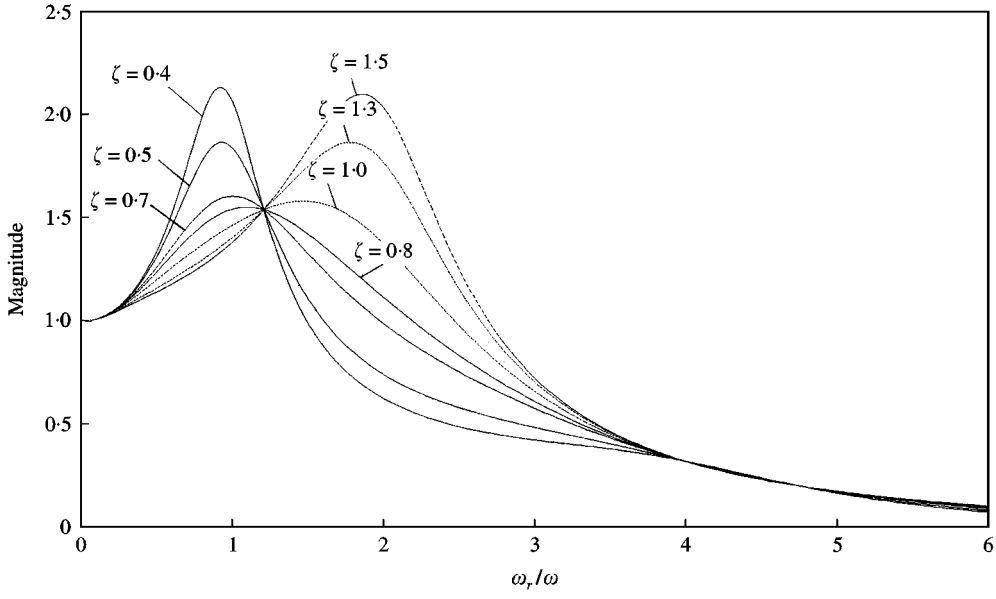

Figure 5. Frequency-response plot for $\mu = \sqrt{4} = 2$, $\lambda = 2$.

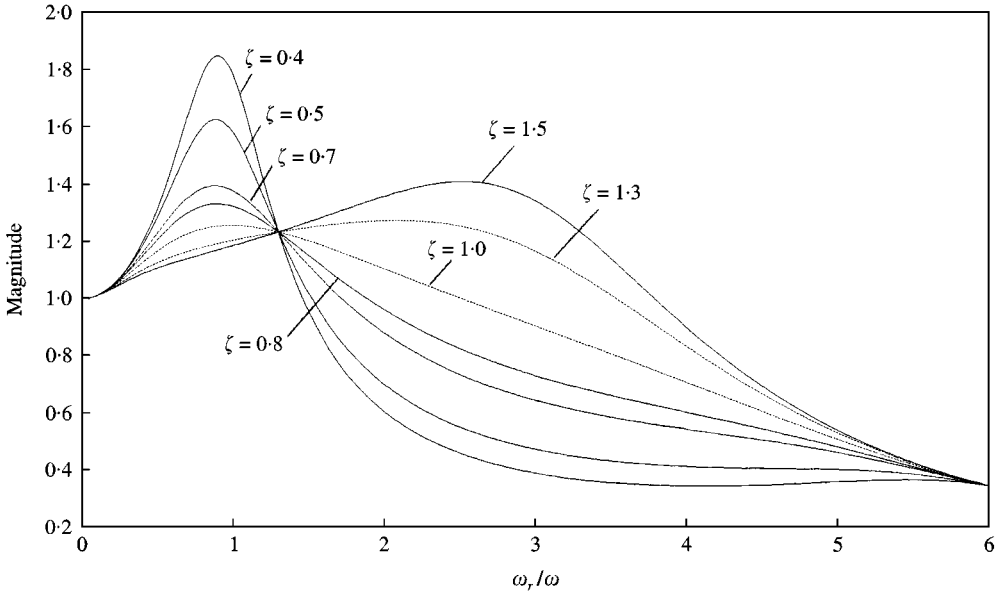

Figure 6. Frequency-response plot for $\mu = \sqrt{4} = 2$, $\lambda = 3$.

the response shifts to the right with increasing values of λ. In Figure 8 maximum magnitude curves are plotted for different μ values. Again similar observations can be made. For increasing values of μ, maximum magnitudes are decreased and also the minima of the curves are shifted to the right. Another observation is that for increasing values of λ and μ the response magnitudes are lowered and the minimum disappears. In Figure 9 the frequency response of the rigid control system is shown which means that $\lambda = \infty$. The

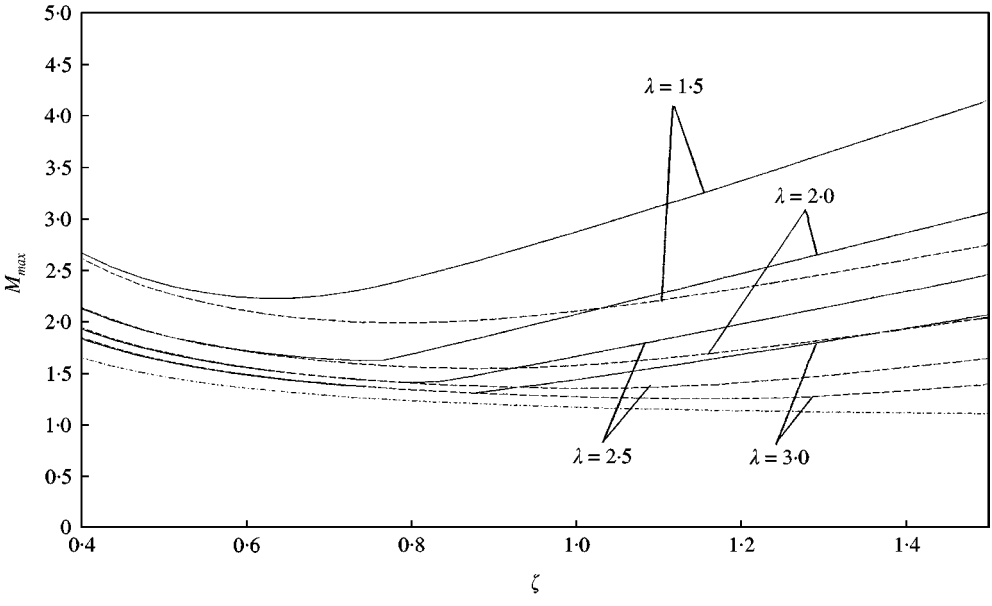

Figure 7. Maximum magnitude plots, solid line plot is for $\mu = \sqrt{2} = 1{\cdot}41$, dashed line plot is for $\mu = \sqrt{5} = 2{\cdot}24$.

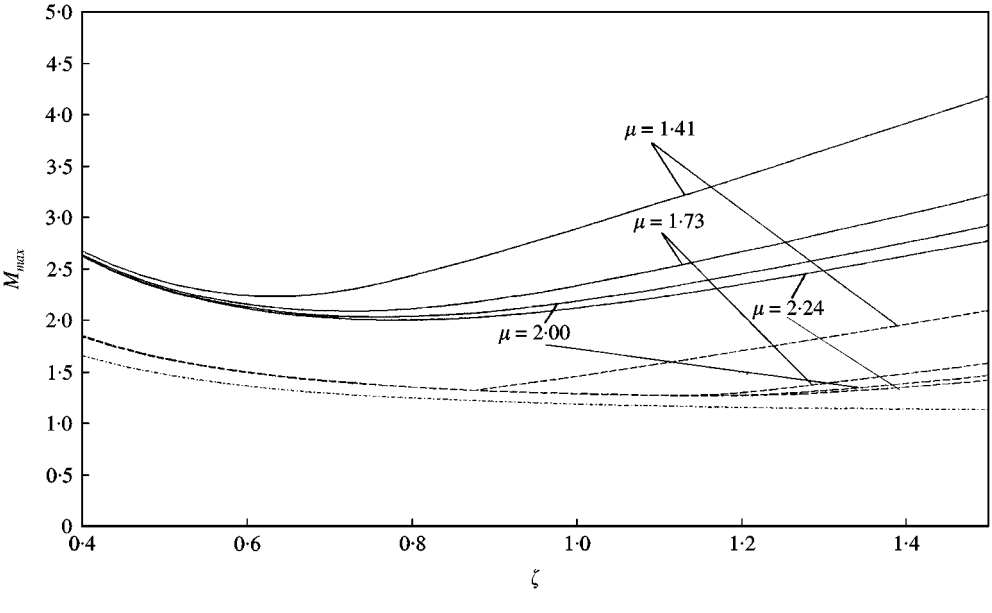

Figure 8. Maximum magnitude plots, solid line plot is for $\lambda = 1{\cdot}5$, dashed line plot is for $\lambda = 3$, and dash-dot line plot is for $\lambda = \infty$.

second peak which was observed in the plots of Figure 6 disappears when $\mu > 2$ and $\lambda > 6$. The elastic control system behaves like a rigid system and the system is no longer excited at the structural frequency ω_n and at substructural frequency ω_L. Figures 10 and 11 show the phase angle plots and the phase angle versus magnitude plots respectively. In Figure 12 the plot of Figure 11 is repeated and compared with the frequency response whilst structural damping exists. The structural damping $\zeta_n = 0{\cdot}02$. The effect of the structural damping is

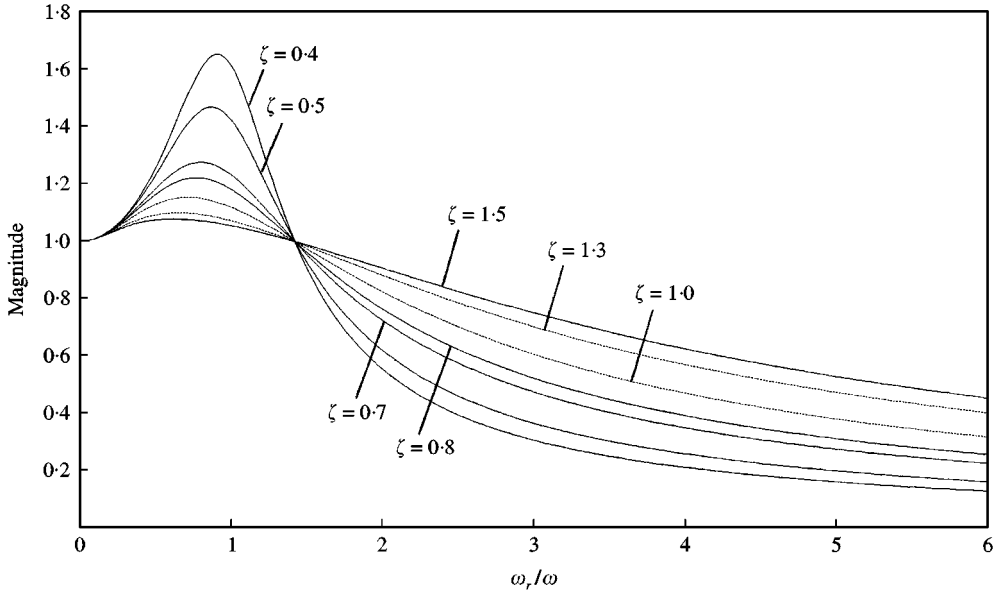

Figure 9. Frequency-response plot for rigid control system.

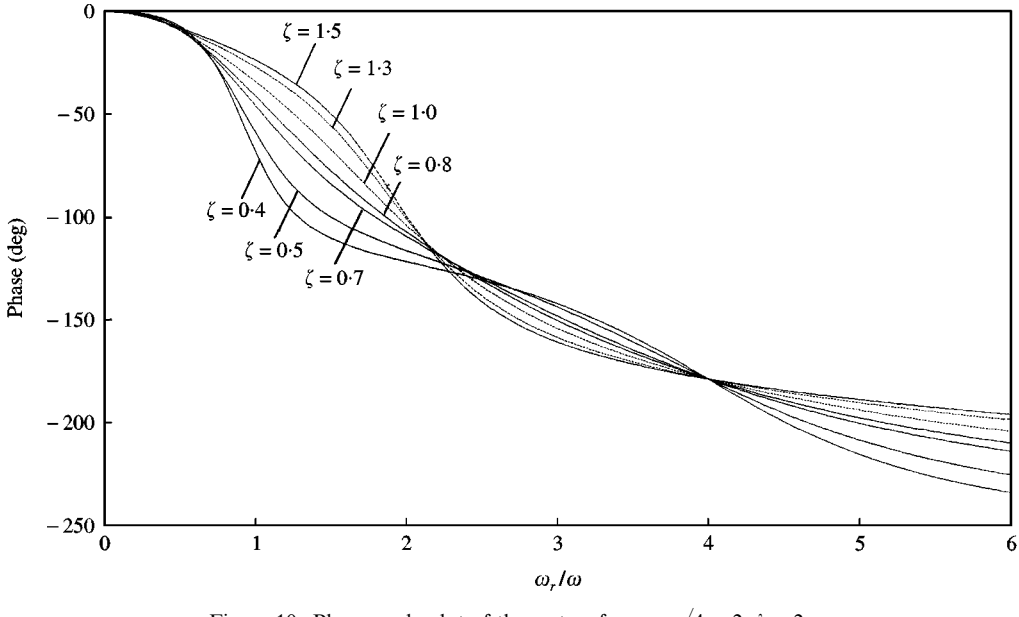

Figure 10. Phase angle plot of the system for $\mu = \sqrt{4} = 2$, $\lambda = 2$.

negligible for low values of control damping ζ and more effective at high values. The overall behaviour of the system is only slightly affected by the structural damping.

3. TRAJECTORY TRACKING

If the elastic control system has to follow a certain trajectory, a possible trajectory for this purpose is the cycloidal function commonly used in cam design. Since the cycloidal

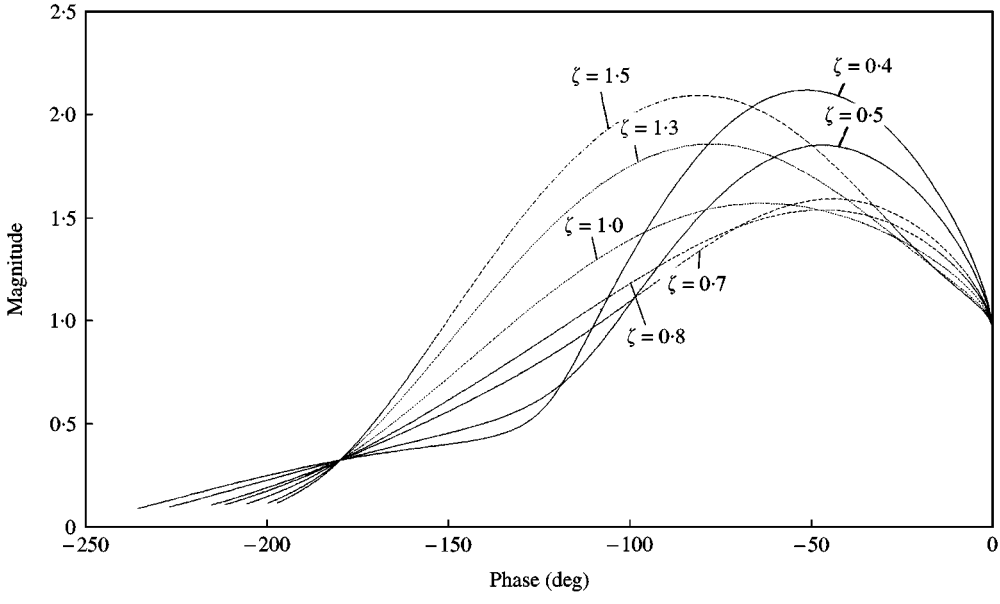

Figure 11. Phase angle versus magnitude plot for $\mu = \sqrt{4} = 2$, $\lambda = 2$.

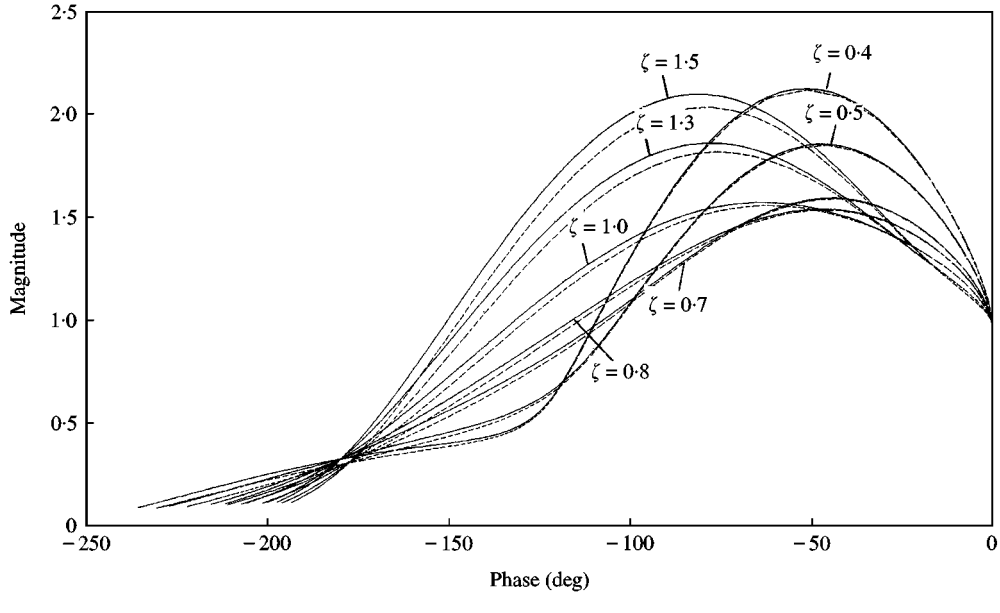

Figure 12. Phase angle versus magnitude plot for $\mu = \sqrt{4} = 2$, $\lambda = 2$. Solid line plot is for the system without structural damping, dashed line plot is for the system with structural damping $\zeta_n = 0{\cdot}02$.

function, when derived twice with respect to time, give a pure sinusoidal acceleration which is zero at the beginning and at the end, it is well suited, especially in robotics applications, as a servomotor motion trajectory for smooth running. The cycloid has two parts: one is ramp and the other is sinusoid:

$$\theta(t) = \frac{\theta_d}{t_r}\, t - \frac{\theta_d}{2\pi} \sin \frac{2\pi}{t_r}\, t = \frac{\theta_d}{2\pi} (\omega_r t - \sin \omega_r t), \quad \omega_r = \frac{2\pi}{t_r}. \tag{23}$$

Here $\theta(t)$ is the trajectory, θ_d is the desired angle travelled, t_r is the rise time for the angle travelled, and ω_r is the rise frequency. Suppose an elastic control system has the values $\mu = 2$, $\lambda = 2$, $\zeta = 0{\cdot}4$, $\omega = 70$ rad/s, and the resonance frequency ratio is $r = \omega_r/\omega = 0{\cdot}6$. To examine the steady state error of the control system to each part of the cycloidal input, the Laplace transform of the cycloidal trajectory is obtained as

$$\theta(s) = \frac{\theta_d \omega_r}{2\pi}\left[\frac{1}{s^2} - \frac{1}{s^2 + \omega_r^2}\right]. \tag{24}$$

The Laplace transform of the error $E(s)/\theta_d(s)$ can also be found as

$$\frac{E(s)}{\theta_d(s)} = \frac{s^2\left[\left(\dfrac{1}{\mu^2\omega_L^2}\right)s^2 + \left(\dfrac{1}{\omega_L^2}2\zeta\omega\right)s + \left(1 + \dfrac{\omega^2}{\omega_L^2}\right)\right]}{\left[\left(\dfrac{1}{\mu^2\omega_L^2}\right)s^4 + \left(\dfrac{1}{\omega_L^2}2\zeta\omega\right)s^3 + \left(1 + \dfrac{\omega^2}{\omega_L^2}\right)s^2 + (2\zeta\omega)s + \omega^2\right]}. \tag{25}$$

Here the $\beta = z/\omega \approx 1/2\zeta$ approximation is used and ζ_n is neglected. If the final value theorem

$$e_{ss} = \lim_{s \to 0} sE(s) \tag{26}$$

is used, the steady state error of the system for the cycloidal input is found to be zero. However, for the sinusoidal part of the input, the output will have a different magnitude and phase angle. That is why, for regular cycloidal input, zero steady state error and precise trajectory tracking cannot be reached as can be seen in Figures 13 and 14. If the sinusoidal input is modified so that phase is eliminated and magnitude is adjusted, it may be possible to obtain zero steady state error and good tracking. The proposed modified cycloidal input function is

$$\theta(t) = \frac{\theta_d}{2\pi}\left[\omega_r t - \frac{1}{M(r, \zeta, \lambda, \mu)}\sin(\omega_r t + \phi(r, \zeta, \lambda, \mu))\right]. \tag{27}$$

For a chosen ζ, r, λ and μ, the magnitude M and the phase angle ϕ are known from equation (16). When these values are inserted into the modified cycloidal input, the sinusoidal output of the control system will be equal to the desired sinusoidal part of the cycloidal input and better tracking is expected. To show the effectiveness of the proposed method, two examples are given. In the first example $\zeta = 0{\cdot}4$ is chosen (low damping), $\mu = 2$ and $\lambda = 2$; this means that the control system is highly elastic. For these values $M = 1{\cdot}565$ and $\phi = 0{\cdot}2166$ rad. Results are shown in Figure 15. The dashed line plot is the response of the elastic control system to the cycloidal input, and dash-dot line is the response of the elastic control system to the modified cycloidal input. The system follows the modified input precisely but a small lag at the beginning and a small residual vibration at the end is observed. The reason for this can be explained as follows. Since the modified cycloidal function is defined by the finite internal $0 \leqslant t \leqslant t_r$, it should actually be written as

$$\theta(t) = \frac{\theta_d}{2\pi}\left[\omega_r t - \frac{1}{M}\sin(\omega_r t + \phi)\right][u(t) - u(t - t_r)] + \theta_d u(t - t_r), \tag{28}$$

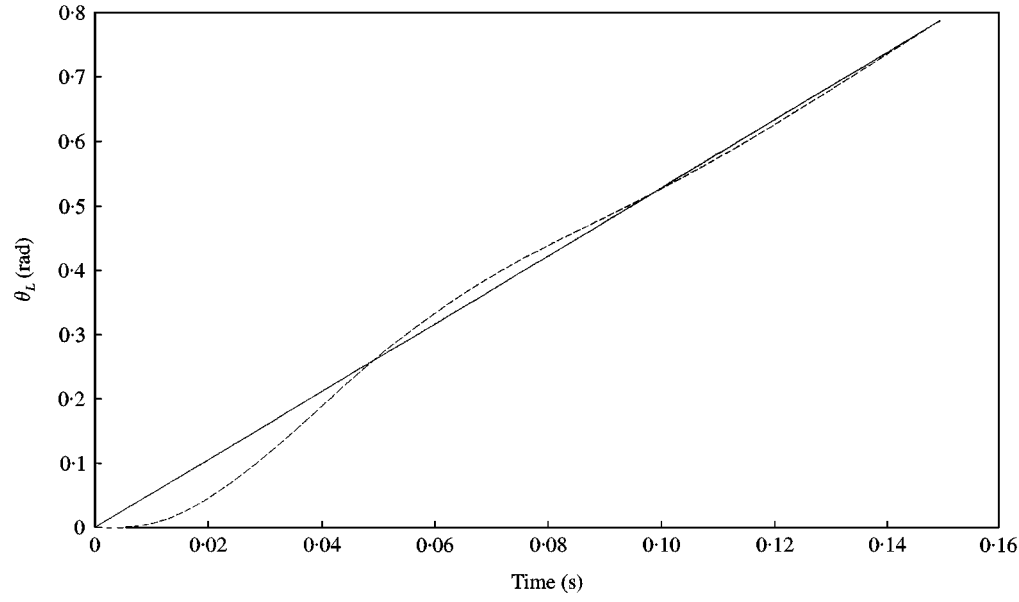

Figure 13. System response to the ramp part of the cycloidal input, $\zeta = 0{\cdot}4$, $\lambda = 2$, $\mu = 2$, —— $r = 0{\cdot}6$, — input; – – – output.

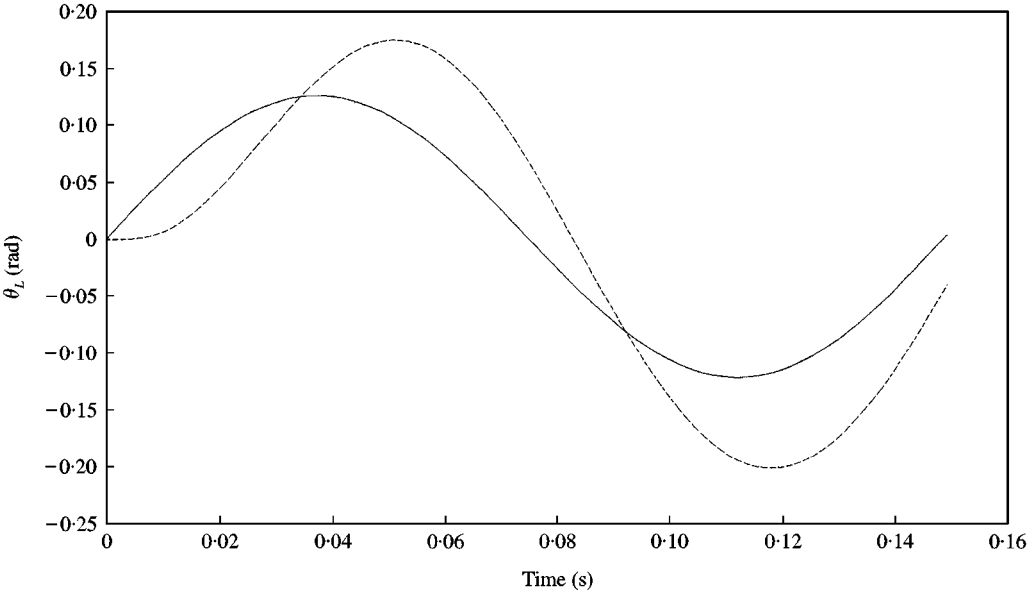

Figure 14. System response to the sinusoid part of the cycloidal input, $\zeta = 0{\cdot}4$, $\lambda = 2$, $\mu = 2$, $r = 0{\cdot}6$. ——Input; – – – output.

where $u(t)$ is the unit step function. It is seen that there are step changes at $t = 0$ and at $t = t_r$, that is,

$$\theta(0^+) - \theta(0^-) = -\frac{\theta_d \sin\phi}{2\pi M}, \qquad \theta(t_r^+) - \theta(t_r^-) = \frac{\theta_d \sin\phi}{2\pi M}. \tag{29}$$

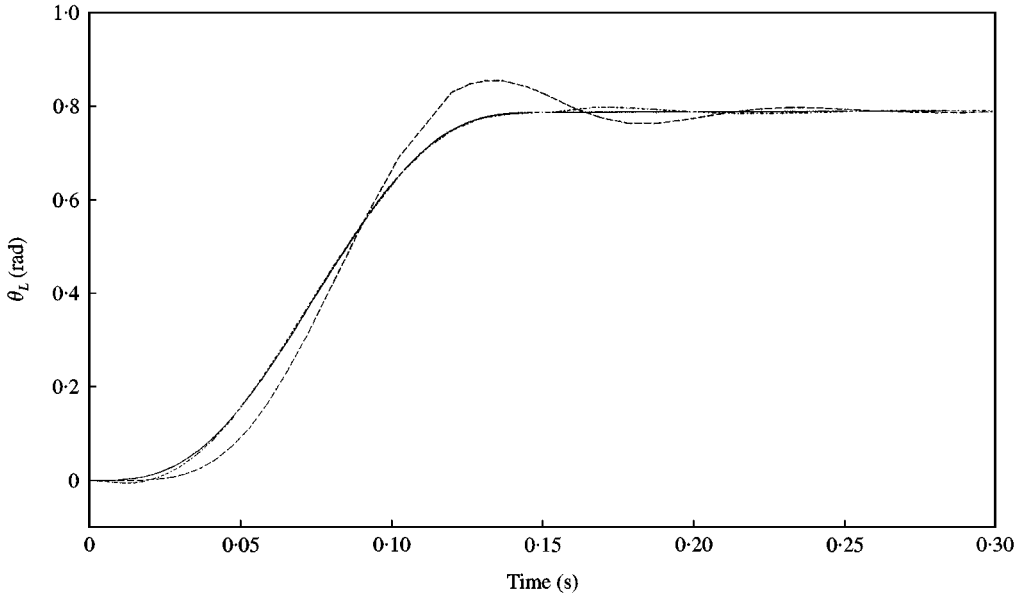

Figure 15. System response to the cycloidal input, $\zeta = 0{\cdot}4$, $\mu = 2$, $\lambda = 2$, $r = 0{\cdot}6$. Dashed line plot is the system response to the cycloidal input, dash-dot line plot is the system response to the modified cycloidol input.

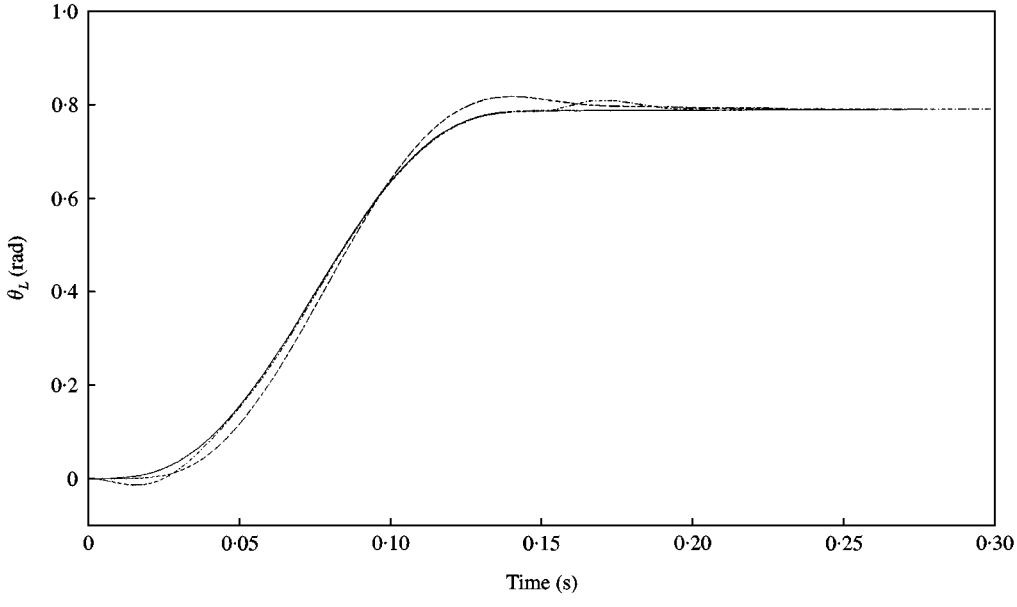

Figure 16. System response to the cycloidal input, $\zeta = 1{\cdot}5$, $\mu = 2$, $\lambda = 2$, $r = 0{\cdot}6$. Dashed line plot is the system response to the cycloidal input, dash-dot line plot is the system response to the modified cycloidol input.

Because of these step changes a lag at the beginning and a residual or transient vibration at the end is expected. For the examples chosen these impulsive effects of the modified cycloidal input are not discouraging and the response is much better and more acceptable than the unmodified cycloidal input. The lower the value of $\sin \phi$ and the bigger the value of 2πM, the smaller the effect which these step changes will have on the system. In the second

example $\zeta = 1{\cdot}5$ (a high damping) and again $\lambda = 2$, and $\mu = 2$. For these values $M = 1{\cdot}190$, and $\phi = -0{\cdot}1787$ rad. Figure 16 shows the responses of the control system to the cycloidal and modified cycloidal inputs. Again the system follows the input precisely with some lag and residual vibration. Since this time the value of M is less than that in the previous example, the step change is bigger, and consequently the lag and residual vibration amplitude are also greater. For both cases $r = 0{\cdot}6$ or $t_r = 0{\cdot}1496$ s. Up to the value $r = 0{\cdot}3$, for any ζ, the phase angle is very small and the system tracks the input with negligible lag and residual vibration. The plot in Figure 3 shows the magnitude of M with respect to the ratio r which is between the cycloidal frequency and the control frequency. For a low frequency ratio r and low control damping ζ, and for high frequency ratio r and high control damping ζ, M assumes large values. Since large values of M will lower the step changes, and consequently the magnitude of the lag and transient vibration will be lower. With high frequency ratios or with low frequency ratios high or low control damping respectively, should be used to obtain large M values it should also be noticed that for low values of λ the range of frequency ratio r narrows. Higher λ values should also be preferred. These two extreme examples show that even with an elastic control system, it is possible to obtain fast and precise tracking for the cycloidal input.

4. CONCLUSION

An elastic control system consisting of a servomotor, elastic shaft and a rigid manipulator link is studied. The transfer function of the control system is obtained, including parameters related to the flexibility of the system. The frequency response of the system is analyzed and the effect of parameters such as substructural frequency ratio λ, structural frequency ratio μ and resonance frequency ratio r on the system response are studied. It is shown that for low values of control system damping ζ, the system is affected by the control system frequency ω and by the structural frequency ω_n. For increasing values of ζ, the control system is affected only by the substructural frequency ω_L. Control system damping ζ acts as a measure of the boundary condition at the motor side. When ζ is zero, the motor side is free; when it is infinite, the motor side is clamped. If $\mu > 2$ and $\lambda > 6$, the elastic control system behaves as a rigid control system and only the control frequency ω is effective. A modified cycloidal input function is proposed for the elastic control system to track precisely a trajectory, and it is shown that, although the system is highly elastic, with the proper selection of the rise time, which is a function of λ and μ, it may track the input precisely.

REFERENCES

1. R. H. CANNON and D. E. ROSENTHAL 1984 *AIAA Journal of Guidance, Control and Dynamics* **7**, 546–553. Experiments in control of flexible structure with noncolocated sensors and actuators.
2. W. J. BOOK 1993 *ASME Journal of Dynamic Systems, Measurement, and Control* **115**, 252–261. Controlled motion in an elastic world.
3. S. P. BHAT and D. K. MIU 1990 *ASME Journal of Dynamic Systems, Measurement, and Control* **112**, 667–674. Precise point to point positioning control of flexible structure.
4. R. LOZANO and B. BROGLIATO 1996 *IEEE Transactions on Automatic Control* **37**, 174–181. Adaptive control of robot manipulator with flexible joints.
5. M. W. SPONG 1987 *ASME Journal of Dynamic Systems, Measurement and Control* **109**, 310–319. Modeling and control of elastic joint robots.
6. R. MARINO and M. W. SPONG 1986 *IEEE International Conference on Robotics and Automation, San Francisco, CA*, 1026–1030. Nonlinear control techniques for flexible joint manipulators: a single link case study.

7. P. TOMEI, S. NICOSIA and A. FICOLA 1986 *IEEE International Conference on Robotics and Automation*, *San Francisco*, *CA*. An approach to the adaptive control of elastic joint robots.
8. Y. DOTE and D. AKHMETOV 1995 *International Conference on Recent Advances in Mechatronics*, *Istanbul*, *Turkey*, 1150–1155. Adaptive vibration suppression control for torsional system driven by fuzzy robust ac drive system.
9. O. SATO, H. SHIMAJIMA and T. KANEKO 1987 *JSME International Journal* **30**, 1465–1472. Positioning control of a gear train system including flexible shafts.
10. H. DIKEN 1996 *AIAA Journal of Guidance*, *Control and Dynamics* **19**, 715–718. Precise trajectory tracking control of elastic joint manipulator.
11. A. ANKARALI and H. DIKEN 1997 *Journal of Sound and Vibration* **204**, 162–170. Vibration control of an elastic manipulator link.
12. K. S. FU, R. C. GONZALES and C. S. G. LEE 1987 *Robotics*: *Control*, *Sensing*, *Vision*, *and Intelligence*. New York: McGraw-Hill.
13. K. OGATA 1990 *Modern Control Engineering*. Englewood Cliffs, NJ: Prentice-Hall.